All-optical High Speed Logic Gates Using SOA

M. Sahafi, A. Rostami, A. Sahafi

Faculty of Electrical and Computer Engineering
University of Tabriz, Tabriz 51666, Iran
ms.mahdi@yahoo.com , ali.sahafi88@ms.tabrizu.ac.ir

Abstract

In this paper a novel and simple structure for operation as a high speed optical logic gate based on bulk semiconductor optical amplifier (SOA) is presented. The gain dynamic and phase response of bulk SOA using rate equations including the dynamics of carrier heating (CH) and spectral-hole burning (SHB) numerically is investigated. By using the presented numerical method, operation of NOR gate is analyzed and we show that the NOR gate can operates at 1Tb/s. High speed logic gates based on bulk SOA can be realized by using the proposed structure.

1. Introduction

Optical logic gates, such as all-optical NOR, NAND and XOR gates are key and important elements for all-optical signal processing. All-optical logic gates fundamentally works on nonlinear characteristics of medium. So far, some methods utilizing the nonlinear operation of optical fiber and semiconductor optical amplifier (SOA) have been used to demonstrate all-optical functions. The all-optical logic gate based on nonlinear characteristics of optical fiber has the potential of operating at terabits per second due to very short relaxation times (<100 fs) of its nonlinearity. The disadvantages of optical fiber are its weak nonlinearity, long interaction lengths and high control energy that is required to achieve reasonable switching efficiency. But, semiconductor optical amplifier has the advantages of high nonlinearity and it is simple for integration to operate as logic gates. All optical XOR gates at speeds of 20 to 40 Gb/s have been demonstrated with Semiconductor Laser Amplifier Loop Mirror (SLALOM) [1, 2], Ultrafast Nonlinear Interferometer (UNI) [3], and SOA based Mach-Zehnder interferometer (SOA-MZI) [4]. The all-optical logic gate base on SOA-MZI is believed to be stable, compact and simple. However, the operating speed of XOR is limited to ~ 250 Gb/s due to the response time of gain saturation in a quantum dot SOA [5]. In this paper, we simulated the high performance optical logic gate, based on output chirping in the SOA. On the other word, we use instantaneous change in phase of propagating optical pulse for logic operation. Using phase variation, eliminates the response time limitation of gain saturation and operating speed can reach more than one tera bit per second.

In this paper, we examine this idea theoretically and present some simulated results evaluated numerically. A principle of operation is presented in section 2. In section 3, SOA model is discussed. In section 4, the optical filter model is illustrated. Finally the simulation results are illustrated and discussed in section 5.

2. Principle of Operation

The proposed structure for logic gate consists of one SOA, one Passive Optical Filter (POF) and two couplers. A continuous wave (CW) beam is injected into the CW port of SOA as illustrated in Fig. 1. According to conventional operation of light propagation through bulk SOA, after a few nano second steady state condition is obtained. Two optical control beams are sent into port A and B of the gate. The wavelengths of the two input signals can be same or different. Input signals from A and B enter the first coupler and combine with CW in second coupler. These combined waves then enter the SOA. Existence or non existence of data stream A and B, cause different chirping for CW. Optical filter eliminates undesirable part of SOA's output wave and pass others to obtain logic operation. To perform the NOR function as shown in the Table 1, optical filter is a high pass filter.

When A= 0 and B=0, the SOA output signal is in highest optical frequency (positive chirping) and must pass through designed optical filter and output become “1”. In other situations, output signal is in lower optical frequency and is eliminated by optical high pass filter. Thus, output will be on “0” state. In this paper, we use a simplified dynamic model, and the rate equations for carrier density in an SOA were derived and solved for gain and phase recovery. The analysis is then extended to include the nonlinear effects of carrier heating (CH) and spectral hole burning (SHB).

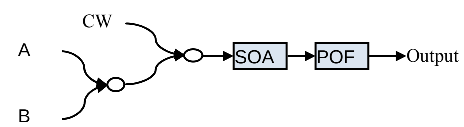

Fig. 1. Basic configuration of proposed logic gate

Table 1. Truth table of NOR operation

Data A	Data B	NOR
0	0	1
0	1	0
1	0	0
1	1	0

3. SOA Model

In simulation step, we consider InGaAsP on InP substrate that is studied more as material for semiconductor optical amplifiers. For simplicity, we assume an ideal facet and neglect the amplified spontaneous emission (ASE) in calculation for simulation. The propagation of an electromagnetic field inside the amplifier is governed by the wave equation:

$$\nabla^2 \vec{E} - \frac{\varepsilon}{c^2}\frac{\partial^2 \vec{E}}{\partial t^2} = 0 \tag{1}$$

The dielectric constant is given by:

$$\varepsilon = n_b^2 + \chi \ , \tag{2}$$

$$\chi(n) = -\frac{\overline{n}c}{\omega_0}(\alpha + i)g(n) \tag{3}$$

where n_b, χ, $\overline{n}$, ω_0, and α are the background refractive index , the susceptibility, the effective mode index, the photon angular frequency and the line-width enhancement factor respectively. The optical gain, $g(n)$, approximately given as:

$$g(n) = a(n - n_{tr}) \ , \tag{4}$$

where a is the gain constant, *n* is the injected carrier density and n_{tr} is the carrier density needed for transparency. The carrier induced refractive index variation is accounted for using the line-width enhancement factor (α), which is the ratio of the change in real part of refractive index to the imaginary part of it. The typical value of α, is in the range of 3 to 8. The electric field E(x,y,z,t) can be written as [1]:

$$\vec{E}(x,y,z,t) = \hat{\varepsilon}\frac{1}{2}\{\phi(x,y)A(z,t)\exp[i(k_0 z - \omega_0 t)]\} \ , \tag{5}$$

where $\hat{\varepsilon}$ is the polarization unit vector, $k_0 = \overline{n}\omega_0/c$ and, A(z,t) is the slowly varying amplitude of the propagating wave. Using above equations and neglecting second derivatives of A(z,t) with respect to t and z, and integrating over the transverse dimensions x and y, we obtain the following equations as [1]:

$$\frac{\partial^2 \phi}{\partial x^2} + \frac{\partial^2 \phi}{\partial y^2} + (n_b^2 - \overline{n}^2)\frac{\omega_0^2}{c^2}\phi = 0 \ , \tag{6}$$

$$\frac{\partial A}{\partial z} + \frac{1}{v_g}\frac{\partial A}{\partial t} = \frac{i\omega_0 \Gamma}{2\overline{n}c}\chi A - \frac{1}{2}\alpha_{\mathrm{int}} A \ , \tag{7}$$

$$v_g = \frac{c}{n_g} \ , \tag{8}$$

$$n_g = \overline{n} + \omega_0\left(\frac{\partial \overline{n}}{\partial \omega}\right) \ , \tag{9}$$

where υ_g is the group velocity, Γ is the confinement factor and α_{int} is the internal loss.

The evolution of carrier density, n, can be described by the following equation [1]:

$$\frac{\partial n}{\partial t} = \frac{I}{eV} - \frac{n}{\tau_c} - \frac{\Gamma g(n)}{dw\hbar\omega_0}|A|^2 \ , \tag{10}$$

In (10), V is the volume of the active region, I is the injected current, e is the charge of the electron, τ_c is the carrier lifetime, d is the depth and w is the width of the active region. For pulse propagation, (7) and (10) can be further simplified by using the retarded time frame:

$$\tau = t - \frac{z}{\upsilon_g} \ , \tag{11}$$

We assume:

$$A(z,\tau) = \sqrt{P(z,\tau)}e^{j\phi(z,\tau)} \ , \tag{12}$$

where P(z, τ) and φ(z, τ) are the instantaneous power and the phase of the propagating pulse respectively. Using (3) to (12), we obtain the following coupled equations:

$$\frac{\partial g}{\partial \tau} = -\frac{g - g_0}{\tau_c} - \frac{gP}{E_{sat}} \ , \tag{13}$$

$$\frac{\partial P}{\partial z} = (\Gamma g - \alpha_{\mathrm{int}})P \ , \tag{14}$$

$$E_{sat} = \frac{\hbar\omega_0 dw}{\Gamma a} \ , \tag{15}$$

$$g_0 = a\left(\frac{I\tau_c}{eV} - n_{tr}\right) \ , \tag{16}$$

We now introduce two additional equations managing gain dynamic, induced by carrier heating and spectral hole burning effects as follows [6]:

$$\frac{\partial g_{SHB}}{\partial \tau} = -\frac{g_{SHB}}{\tau_{SHB}} - \frac{\varepsilon_{SHB}}{\tau_{SHB}} g_{tot} P(\tau,z) - \frac{\partial g_l}{\partial \tau} - \frac{\partial g_{CH}}{\partial \tau} \ , \tag{17}$$

$$\frac{\partial g_{CH}}{\partial \tau} = -\frac{g_{CH}}{\tau_{CH}} - \frac{\varepsilon_{CH}}{\tau_{CH}} g_{tot} P(\tau,z) \ , \tag{18}$$

where τ_{SHB} is the carrier-carrier scattering rate while τ_{CH} is the temperature relaxation rate. ε_{SHB} and ε_{CH} are the nonlinear gain suppression factors due to spectral hole burning and carrier heating respectively [6]. Hereinafter, we use $g_l(\tau)$ and α_l instead of g(τ) and α, then the total gain is given by:

$$g_{tot}(\tau) = g_l(\tau) + g_{CH}(\tau) + g_{SHB}(\tau) \ , \tag{19}$$

Solution of (14) with neglecting internal loss is:

$$P(\tau, L) = P(\tau,0)\exp(h_{tot}(\tau)) \ , \tag{20}$$

where

$$h_{tot}(\tau) = \Gamma\int_0^L g_{tot}(\tau,z)dz \ , \tag{21}$$

and $h_{tot}(\tau)$ is the total integrated net gain, $h_l(\tau)$, $h_{SHB}(\tau)$ and $h_{CH}(\tau)$ are the integrated net gain due to linear gain, spectral hole burning and carrier heating respectively. Integrating over both sides of (13), (17), (18) and using:

$$h_l(\tau) = \Gamma\int_0^L g_l(\tau,z)dz \ , \tag{22}$$

$$h_{SHB}(\tau) = \Gamma \int_0^L g_{SHB}(\tau, z) dz \ , \tag{23}$$

$$h_{CH}(\tau) = \Gamma \int_0^L g_{CH}(\tau, z) dz \ , \tag{24}$$

we obtain:

$$\frac{\partial h_l}{\partial \tau} = \frac{\Gamma g_0 L - h_l}{\tau_c} - [\exp(h_{tot}) - 1] \frac{P_{in}(\tau)}{E_{sat}} , \tag{25}$$

$$\frac{\partial h_{SHB}}{\partial \tau} = -\frac{h_{SHB}}{\tau_{SHB}} - \frac{\varepsilon_{SHB}}{\tau_{SHB}} [\exp(h_{tot}) - 1] P_{in}(\tau) - \frac{\partial h}{\partial \tau} - \frac{\partial h_{CH}}{\partial \tau} , \tag{26}$$

$$\frac{\partial h_{CH}}{\partial \tau} = -\frac{h_{CH}}{\tau_{CH}} - \frac{\varepsilon_{CH}}{\tau_{CH}} [\exp(h_{tot}) - 1] P_{in}(\tau) , \tag{27}$$

The optical gain as a function of time can be numerically solved considering coupled equations (25)–(27).

The time dependence phase is given as follows [6]:

$$\phi(\tau) = -\frac{1}{2}(\alpha_l h_l(\tau) + \alpha_{CH} h_{CH}(\tau)) \ , \tag{28}$$

A time dependent phase variation leads to a variation in optical frequency content of the propagating pulse. The instantaneous variation in frequency, known as the frequency chirp $\Delta\nu(\tau)$ is given by [6]:

$$\Delta \nu(\tau) = -\frac{1}{2\pi} \frac{d\phi}{d\tau} = \frac{1}{4\pi} (\alpha \frac{dh}{d\tau} + \alpha_{CH} \frac{dh_{CH}}{d\tau}) \ , \tag{29}$$

and frequency of output of SOA is:

$$f_{out}(\tau) = f_{in}(\tau) + \Delta \upsilon(\tau) \ , \tag{30}$$

We use this phenomenon to produce logic operation in this paper.

4. Optical Filter Model

For simplicity, we use the following equation for modeling of Optical filter.

$$H(\omega) = \exp(-\ln 2 \times (\frac{\omega - \omega_C}{\Delta\omega/2})^4) \ , \tag{31}$$

where ω_c and $\Delta\omega$ are the central frequency and the full width at half maximum value of $H(\omega)$. If we want to show the operation on frequency domain, the following curve should be considered (Fig. 2).

It should mention that ω_{rf} is difference frequency between 1% and 99% of maximum value of $H(\omega)$. In this simulation, we put $\Delta\omega$ equal to 24GHz and so ω_{rf} is 15GHz.

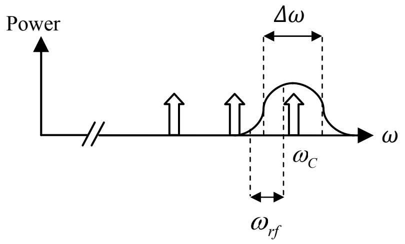

Fig. 2. Operation at frequency domain

5. Numerical Results

We illustrate here the case of logic operation for NOR gate by numerical evaluation of the proposed structure. The input optical signal was set as a Gaussian pulse for logic 1 (Fig. 3).

The investigated device is a typical bulk InGaAsP-InP region with parameters given in table 2 [9] and pumped with 200 mA. Fig. 4 shows 1Tbps process and includes five traces of simulated result. In this figure, (a) and (b) show data streams enters to port A and B. (c) is the output pulse of SOA and (d) is the frequency shifting of output signal. Finally (e) shows the final output after optical filter.

It should mention that in these simulations P_0 is considered to be -5dbm for CW, A and B pulses. In this condition the maximum frequency shifting is 20GHz as shown in (d). Undesirable sections of beam are filtered by designed optical filter and output is exactly NOR function of A and B (Fig. 4.e).

$$P = P_0 \exp(-(\tau/2\tau_0)^2)$$

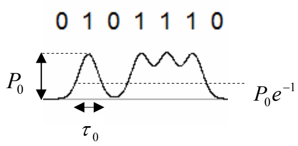

Fig. 3. Data train of A or B

Table 1. Parameters used in simulation

Symbol	Parameter	Value
d	thickness of the amplifier active region	0.2um
w	width of the amplifier active region	2um
L	Length of the amplifier active region	1mm
n_{tr}	carrier density needed for transparency	1.28e+24
a	gain constant	2.75e-20
n_g	group refractive index	3.42
λ	Wave lengh of beam	1.55um
Γ	confinement factor	0.4
α_l	Line-width enhancement factor	7
α_{CH}	Line-width enhancement factor due to carrier heating	1
τ_C	carrier lifetime	250ps
τ_{CH}	carrier temperature relaxation rate	300fs
τ_{SHB}	carrier-carrier scattering rate	100fs
ε_{CH}	gain suppression factor due to carrier heating	0.2/W
ε_{SHB}	gain suppression factor due to spectral hole burning	0.2/W

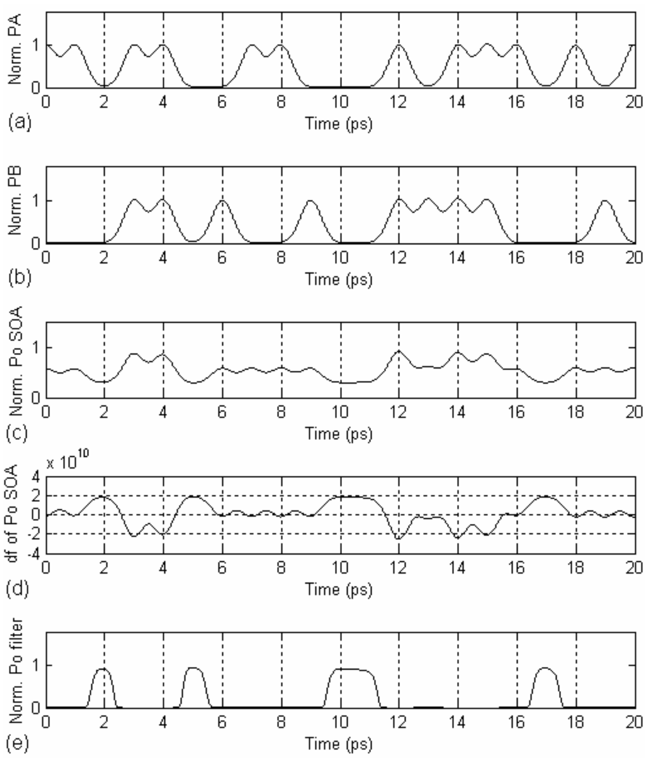

Fig. 4. Simulation results for 1ps pulse width (1Tbps). (a) Input power of port A. (b) Input power of port B. (c) Normalized power of SOA output. (d) Frequency shifting of SOA output. (e) Normalized power of optical filter

6. Conclusions

In this paper, we presented a new promising plan of high speed logic gate using bulk SOA. We have used the nature of SOA to build a NOR logic gate as high speed as 1Tb/s to use in all-optical signal processing. The filter used in this method is simple and practical. Because of using simple model, we can change the characters of the filter to obtain fundamental gates such as XOR and NAND in the future.

7. References

[1] G. P. Agrawal and N. A. Olsson, “Self-Phase Modulation and Spectral Broadening of Optical Pulses in Semiconductor Laser Amplifiers” IEEE J. Quantum Electron. QE-25, 2297 , 1989.

[2] T. Houbavlis, K. Zoiros, A. Hatziefremidis, H. Avramopoulos, L. Occhi, G. Guekos, S. Hansmann, H. Burkhard and R. Dall’Ara, “10 Gbit/s all-optical Boolean XOR with SOA fiber Sagnac gate,” Electron. Lett. 35, 1650-1652 , 1999.

[3] C. Bintjas, M. Kalyvas, G. Theophilopoulos, T. Stathopoulos, H. Avramopoulos, L. Occhi, L. Schares, G. Guekos, S. Hansmann, and R. Dall’Ara, “ 20 Gb/s all-optical XOR with UNI gate,” IEEE Photon. Technol. Lett. 12, 834-836 , 2000.

[4] T. Fjelde, D. Wolfson, A. Kloch, B. Dagens, A. Coquelin, I. Guillemot, F. Gaborit, F. Poingt, and M. Renaud, “Demonstration of 20 Gbit/s all-optical logic XOR in integrated SOA-based interferometric wavelength converter,” Electron. Lett. 36 (22), 1863-1864 , 2000.

[5] H. Sun, Q. Wang, H. Dong and N. K. Dutta “XOR performance of a quantum dot semiconductor optical amplifier based Mach-Zehnder interferometer” OPTICS EXPRESS Vol. 13, No. 6 , 1893 , 2005.

[6] A. Mecozzi and J. Mørk, “Saturation effect in nondegenerate four-wave mixing between short optical pulses in semiconductor laser amplifier,” IEEE J. Sel. Top. Quantum Electron. 3-5, 1190-1207 ,1997.

[7] Wei Yang, Min Zhang, Peida Ye “ Analysis of 160 Gb/s all-optical NRZ-to-RZ data format conversion using quantum-dot semiconductor optical amplifiers assisted Mach-Zehnder interferometer” , Opt. Commun. 2009.

[8] Aghajanpour H, et al. “Ultra-short optical pulse shaping using semiconductor optical amplifier”. Opt Laser Technol, 2008.

[9] J. M. Tang and K. A. Shore “Analysis of the Characteristics of TOAD’s Subject to Frequency-Detuned Control and Signal Picosecond Pulses”, IEEE J. QUANTUM ELECTRONICS, VOL. 35, NO. 11, 1999.